

Pareto Optimal Characterization of a Microwave Transistor

FİLİZ GÜNEŞ¹, AHMET ULUSLU¹, AND PEYMAN MAHOUTI²

¹Department of Electronics and Communication Engineering, Yıldız Technical University—Istanbul, 34467 Istanbul, Turkey

²Department of Electronic and Automation, Vocational School of Technical Sciences, Istanbul Cerrahpaşa University, 34452 Istanbul, Turkey

Corresponding author: Peyman Mahouti (pmahouti@istanbul.edu.tr)

ABSTRACT Herein, noise, gain and port mismatches of a microwave small-signal transistor are expressed as all the set of acceptable Pareto optimal solutions and trade-off relations within the device operation (V_{DS} , I_{DS} , f) domain without any need of expert knowledge of microwave device. In this multi-objective optimization problem, non-dominated sorting genetic algorithm (NSGA) -III is applied to an ultra-low noise amplifier (LNA) transistor NE3511S02 (HJ-FET) where the noise $F_{req} \geq F_{min}$ and output mismatching $V_{outreq} \geq 1$ are preferred as the reference points, while the input mismatching $V_{inopt} \geq 1$ and gain G_{Tmax} are optimized with respect to source Z_S and load Z_L within the unconditionally stable working area. Thus, diverse set of the Pareto optimal (the required noise F_{req} , the optimum input V_{inopt} , the required output V_{outreq} , the maximum transducer gain G_{Tmax}) quadruples are resulted from a fast search of the solution space. Furthermore, the optimum bias condition (V_{DS} , I_{DS}) and sensitivities of the terminations to fabrication tolerances are also determined using the cost analysis in the operation domain for the required P_{max} , I_{DSmax} and performance quadruple. Finally, this work is expected to enable a designer to provide the feasible design target space (FDTS) consisting of all trade-off relations among all the transistor's performance ingredients to be used in the challenging LNA designs.

INDEX TERMS Non-dominated sorting genetic algorithm, Pareto optimal solutions, optimization, impedance mismatching, transducer gain, noise figure.

I. INTRODUCTION

Today ultra-wide band (UWB) transceiver integration requires miniature UWB low noise amplifier (LNA) design with low-power consumption from a low-level battery having high gain, low noise, low input and output voltage standing wave ratio (VSWR). These stringent requirements necessitate a challenging single transistor LNA design optimization. Whatever optimization algorithm and technology are used in this design optimization problem, the most significant ingredient is the feasible design target space (FDTS), since the major challenge in this design problem is to enable the transistor to amplify subject to its physical limitations and trade-off relations among its noise, gain and mismatching at its input and output ports. This FDTS problem has been worked out in the following two stages: (i) Firstly signal and noise parameters of the transistor are modelled throughout its operation domain (V_{DS} , I_{DS} , f) using either the artificial intelligence tools or novel optimization methods using

the limited number of the measurements, in the form of respectively, the black-box or multi-bias equivalent circuit with the typical works respectively, in [1]–[4] and [5]–[7]. In fact these complete modelling methods can also be applied even on the wafer fabricated transistor whose packaging parasitic effects are avoided, since nowadays very accurate S- and noise parameter measurement theory and techniques for on wafer fabricated transistors are available with the typical works [8]–[11]; (ii) The second stage is to solve the transistor's highly nonlinear small-signal performance equations with respect to source (Z_S) and load (Z_L) terminations either analytically or numerically, resulting simultaneous performance ($F_{req} \geq F_{min}$, $V_{in} \geq 1$ (LNA input VSWR), $G_{Tmin} \leq G_T \leq G_{Tmax}$) / ($F_{req} \geq F_{min}$, $V_{out} = 1$ (LNA output VSWR), G_{Tmax}) triplets or ($F_{req} \geq F_{min}$, $V_{in} \geq 1$, $V_{outreq} \geq 1$, $G_{Tmin} \leq G_T \leq G_{Tmax}$) quadruples [12]–[19]. To the best knowledge of the authors, the first time in the literature, ($F_{req} \geq F_{min}$, $V_{in} \geq 1$, $V_{outreq} \geq 1$, $G_{Tmin} \leq G_T \leq G_{Tmax}$) quadruples have been determined by solving the highly nonlinear performance equations of a microwave transistor analytically in [15] and with single-objective (SO)

The associate editor coordinating the review of this manuscript and approving it for publication was Wenjie Feng.

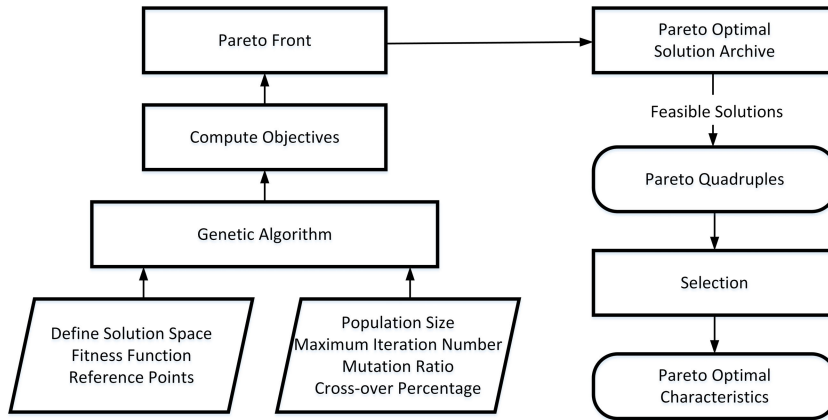


FIGURE 1. NSGA-III for the transistor Pareto optimal characteristics.

multi-objective optimization methods in [19] within its operation (V_{DS} , I_{DS} , f) domain subject to the physical realizability conditions. In these both analytical and optimization methods, the noise $F_{req} \geq F_{min}$ and output mismatching $V_{outreq} \geq 1$ have been preferred as the reference points. In the analytical approach [15], firstly source impedance Z_S has been determined so that the maximum available gain has been ensured for the required noise $F_{req} \geq F_{min}$. Finally the optimum input VSWR V_{inopt} , the corresponding maximum gain G_{Tmax} and the required output VSWR $V_{outreq} \geq 1$ have been achieved using load impedance Z_L as an instrument according to the equality $G_T(Z_S, Z_L) = G_{op}(Z_L) (1 - (|V_{in}| - 1/|V_{in}| + 1)^2 = G_{av}(Z_S) (1 - (|V_{out}| - 1/|V_{out}| + 1))^2$, where $G_{op}(Z_L)$ and $G_{av}(Z_S)$ are the operating and available gain, respectively. Thus, the optimum trade-off relations can be obtained among gain $G_T(f)$, noise $F(f)$, and mismatch losses at the input $V_{in}(f) \geq 1$ and output $V_{out}(f) \geq 1$. However, for the optimization methods, expert knowledge on the transistor’s small-signal and noise performance theory are not needed. In [19], the performance quadruples are obtained solving a single-objective (SO) optimization problem. In other words, all the objectives are aggregated in a single weighted function and solved by novel meta-heuristic intelligent algorithms, which are cuckoo search, differential evolution, fire fly algorithms.

However, an aggregated SO optimization problem has the following limitations (i) The aggregated function leads to only one solution that cannot be guaranteed better than the others; (ii) Trade-offs between objectives cannot be easily evaluated and (iii) The solution may not be attainable unless the search space is convex. On the other hand, multi-objective (MO) optimization problems involve more than one objective function that are to be minimized or maximized; answer is set of solutions that define the best trade-off between competing objectives. Furthermore, Pareto optimal set is the non-dominated solution set that is a set of all the solutions that are not dominated by any member of the solution set.

In literature MO in the sense of Pareto optimality is applied to the problems in the various disciplines from economics to the engineering. Typical works can be given for economic

TABLE 1. Definition of the performance quadruples.

Case	F_{req}	V_{outreq}	V_{in}	G_T , dB
Case-1	F_{min}	1.2	minimum	maximum
Case-2	1.2	1.2		
Case-3	1.3	1.0		
Case-4	1.3	1.1		
Case-5	1.3	1.2		

emission dispatch [20], job shop [21], virtualization network functions (VNF) [22], tuition fees [23], on the power distribution [24], the microwave filter design [25], device modelling and LNA design [26]–[30], and antennas [31], [32].

In this work, our aim is to determine all the set of acceptable Pareto optimal solutions and their trade-off relations of the transistor’s small-signal performance equations within the operation (V_{DS} , I_{DS} , f) domain. For this purpose, user-preference based non-dominated sorting genetic algorithm (NSGA) -III is used, where the noise $F_{req} \geq F_{min}$ and output mismatching $V_{outreq} \geq 1$ are chosen as the reference points. This technique requires less computational resources by performing more focused and guided search rather than approximating entire Pareto optimal front. NSGA-III uses the framework of NSGA-II, but works with a set of supplied or pre-defined reference points and demonstrate its efficacy in solving two-objective to 15 objective optimization problems [33], [34].

NSGA-III is worked out in the study case in following stages:

(i) NE3511S02 [35] is chosen as a test vehicle for which, 10×4050 Pareto optimal solutions are generated in the Pareto archive for 10 different runs of genetic algorithm (GA) for each ($F_{req} \geq F_{min}$, V_{inopt} , G_{Tmax} , $V_{outreq} \geq 1$) quadruple within the region $F_{min} \leq F_{req} \leq 1.3$ and $1 \leq V_{outreq} \leq 1.2$ at each sample frequency between 7GHz - 18GHz. Approximately % 10 of these Pareto optimal (≈ 40500) solutions

TABLE 2. Pareto optimal and analytical results for the ($F_{req} = F_{min}$, V_{inopt} , G_{Tmax} , $V_{outreq} = 1.2$) quadruple of NE3511S02 biased at $V_{DS} = 2V$ and $I_{DS} = 10mA$.

Pareto optimal										Analytical								
f_s , GHz	R_s, Ω	X_s, Ω	R_L, Ω	X_L, Ω	V_{in}	V_{out}	F	G_T , dB	Cost	R_s, Ω	X_s, Ω	R_L, Ω	X_L, Ω	V_{in}	V_{out}	F	G_T , dB	Cost
7	13.371	52.171	23.473	16.367	2.035	2.088	1.268	17.477	3.134	31.665	70.458	39.458	18.675	4.800	1.200	1.057	14.963	4.800
8	10.555	37.927	19.387	21.729	1.786	1.701	1.267	17.058	2.492	27.659	56.908	37.682	16.897	4.000	1.200	1.062	14.229	4.000
9	10.096	23.002	16.892	28.742	1.571	1.357	1.329	16.542	1.992	24.871	45.613	35.090	12.873	3.400	1.200	1.064	13.609	3.400
10	26.118	32.139	35.882	15.709	2.726	1.236	1.099	13.352	2.789	22.794	35.904	33.414	10.943	3.000	1.200	1.072	13.070	3.000
11	22.122	24.652	29.808	10.473	2.531	1.146	1.086	12.875	2.592	21.481	27.156	32.266	9.167	2.700	1.200	1.079	12.625	2.700
12	20.894	14.246	27.911	8.312	2.050	1.198	1.112	12.681	2.078	20.741	19.125	30.889	8.480	2.500	1.200	1.086	12.259	2.500
13	19.057	8.111	26.436	7.429	2.024	1.170	1.111	12.241	2.068	20.716	11.469	29.228	4.273	2.200	1.200	1.096	11.932	2.200
14	20.865	-0.206	25.676	5.554	1.796	1.162	1.126	11.969	1.853	21.443	4.008	28.282	2.200	2.000	1.200	1.107	11.662	2.000
15	21.090	-7.183	22.658	1.205	1.738	1.101	1.139	11.793	1.857	23.241	-3.470	27.361	0.556	1.900	1.200	1.119	11.496	1.900
16	26.098	-13.29	23.704	-1.237	1.883	1.099	1.139	11.466	1.991	26.623	-11.04	26.751	-1.272	1.900	1.200	1.132	11.320	1.900
17	20.088	-25.63	18.448	-4.649	1.615	1.197	1.299	11.987	1.772	32.387	-18.56	26.880	-2.843	2.100	1.200	1.146	11.163	2.100
18	32.817	-30.83	30.226	-8.192	1.820	1.578	1.287	11.479	2.321	42.070	-24.68	28.298	-5.623	2.600	1.200	1.164	11.042	2.600

TABLE 3. Pareto optimal and analytical results for the ($F_{req} = 1.3$, V_{inopt} , G_{Tmax} , $V_{outreq} = 1.1$) quadruple of NE3511S02 biased at $V_{DS} = 2V$ and $I_{DS} = 10mA$.

Pareto optimal										Analytical								
f_s , GHz	R_s, Ω	X_s, Ω	R_L, Ω	X_L, Ω	V_{in}	V_{out}	F	G_T , dB	Cost	R_s, Ω	X_s, Ω	R_L, Ω	X_L, Ω	V_{in}	V_{out}	F	G_T , dB	Cost
9	10.717	26.084	16.095	25.118	1.819	1.197	1.288	16.297	1.928	5.511	22.235	7.217	30.427	2.300	1.100	1.247	17.664	2.354
10	10.226	14.658	15.274	26.227	1.419	1.121	1.330	15.439	1.471	6.610	14.291	9.185	27.499	1.450	1.100	1.271	15.794	1.479
11	10.068	8.551	15.284	21.253	1.260	1.113	1.303	14.548	1.276	6.624	6.988	9.225	23.516	1.200	1.100	1.273	14.757	1.227
12	10.221	0.973	15.067	18.716	1.135	1.108	1.318	13.862	1.162	6.741	0.062	9.345	19.886	1.050	1.100	1.281	13.944	1.069
13	10.078	-4.640	14.179	13.001	1.052	1.103	1.297	13.222	1.058	6.820	-6.591	10.932	16.127	1.200	1.100	1.286	13.214	1.214
14	10.908	-11.15	14.516	9.755	1.017	1.098	1.302	12.699	1.021	6.870	-13.13	10.586	12.286	1.300	1.100	1.289	12.621	1.311
15	10.156	-17.51	12.501	6.105	1.015	1.094	1.309	12.501	1.029	6.977	-18.72	9.481	7.540	1.200	1.100	1.295	12.479	1.205
16	10.304	-23.69	11.442	1.165	1.078	1.127	1.333	12.424	1.138	7.491	-24.59	7.645	2.569	1.100	1.100	1.321	12.503	1.121
17	18.359	-25.78	16.702	-4.956	1.615	1.161	1.319	12.099	1.695	7.012	-31.36	5.792	-2.442	1.600	1.101	1.361	13.285	1.662

are selected as feasible solutions to build up a Pareto front. It should be emphasized that these 40500 Pareto optimal solutions correspond to each single analytical / SO optimized solution at an operation frequency since it contains all the optimal solutions from an “overall” standpoint; unlike SO optimization that may ignore this trade-off viewpoint.

(ii) Thus 5 Pareto optimal characteristics (POCs) are built up using Pareto quadruples within the region $F_{min} \leq F_{req} \leq 1.3$ and $1 \leq V_{outreq} \leq 1.2$, for each of which independent

selection criterion applied to the Pareto optimal solutions within 7GHz - 18GHz bandwidth.

(iii) In order to determine the Pareto optimal solutions, an individual criterion is defined to each Pareto quadruples and the selected solutions are used to build up the POCs of the transistor. Then these POCs are compared with their counterpart analytical characteristics. All these stages can be followed from the flow diagram in Figure 1.

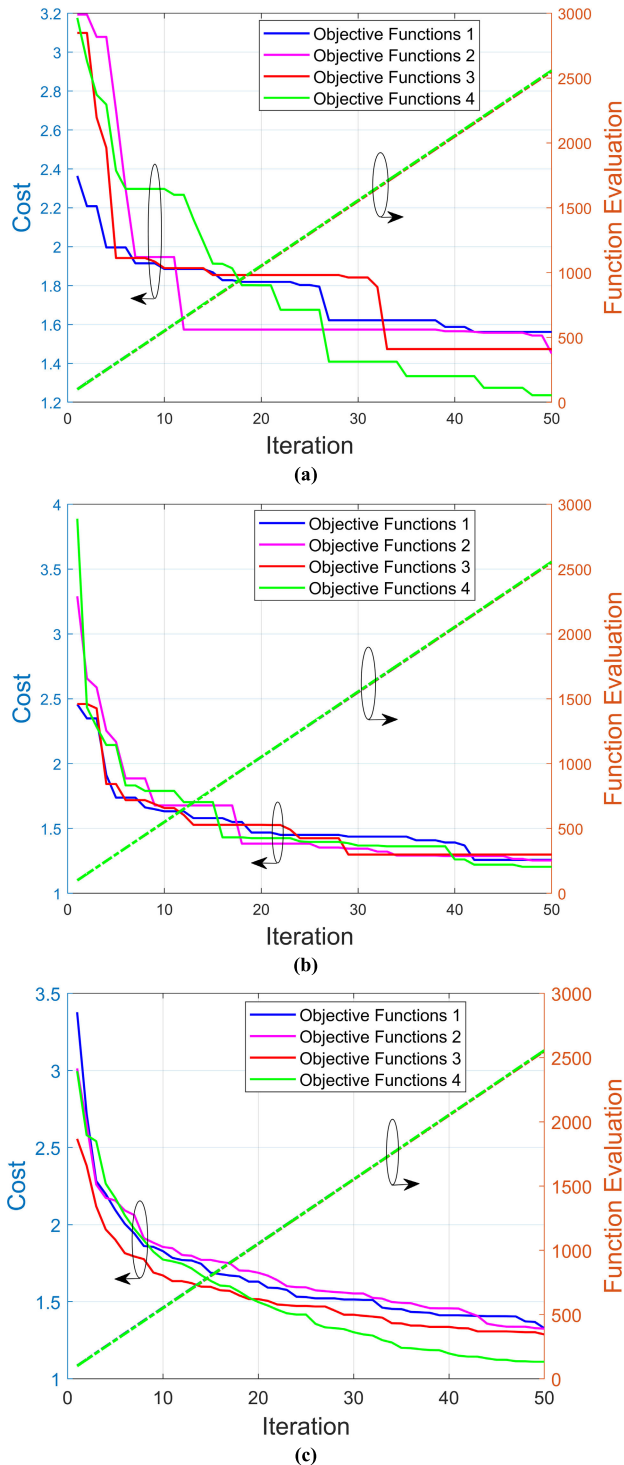


FIGURE 2. Averaged convergence characteristics of the 4 different objective function pairs for the: (A) ($F_{req} = F_{min}, V_{inopt}, G_{Tmax}, V_{outreq} = 1.2$) at 12 GHz, (B) ($F_{req} = 1.2, V_{inopt}, G_{Tmax}, V_{outreq} = 1.2$) at 15GHz, (C) Minimum total cost for ($F_{req} = 1.3, V_{inopt}, G_{Tmax}, V_{outreq} = 1.1$) quadruple over (10 GHz-16GHz), of NE3511S02 at bias condition (2V, 10 mA).

(iv) Besides, the optimum bias condition (V_{DS}, I_{DS}) for a required maximum power dissipation P_{max} , current I_{DSmax} and performance quadruple are determined the minimal total

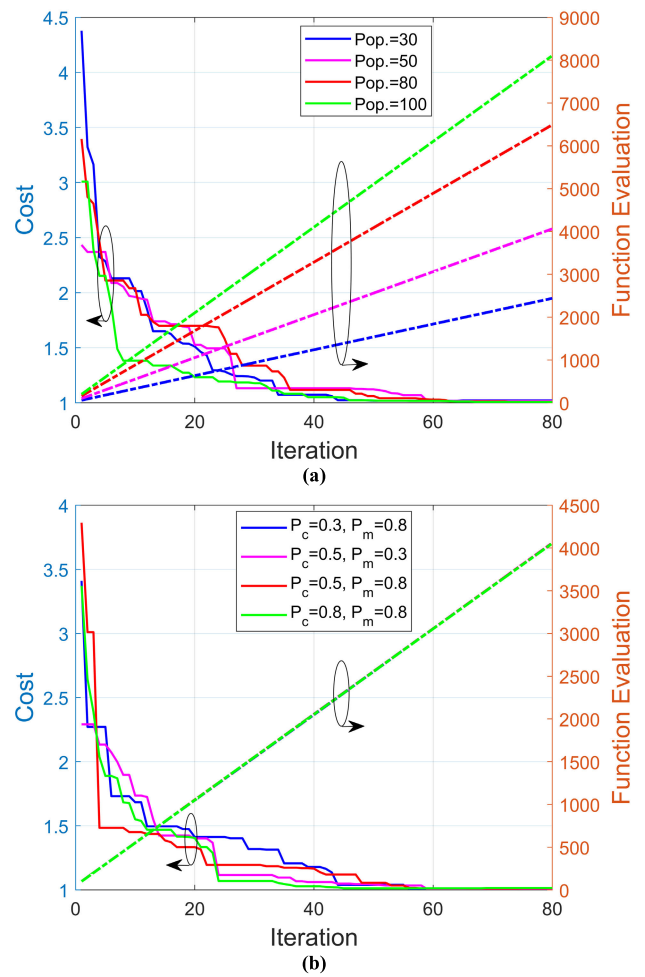


FIGURE 3. Typical cost and FEN variations with iteration for the best performance chosen among 10 runs for ($F_{req} = 1.3, V_{inopt}, G_{Tmax}, V_{outreq} = 1.2$) quadruple, at $V_{DS} = 2V, I_{DS} = 10mA$ and 12GHz: (A) Crossover percentage = 0.5, mutation = 0.5 as population taken as parameter, (B) Population = 50 as crossover (P_c), mutation (P_m), and maximum iteration = 80 are taken as user defined parameters.

cost analysis along the operation bandwidth resulted from the optimizations.

(v) Moreover, Monte Carlo analysis is also made to determine sensitivities of the feasible source and load terminations to fabrication tolerances for a chosen optimal bias condition and performance quadruple.

Linearity evaluation of a small-signal transistor can also be implemented to our GA characterization approach provided that the device's transfer characteristic is defined. Thus, non-linearity for a small deviation around a bias condition can be expressed by a Taylor series and neglecting terms with the higher than third degree, 1dB compression point (PL1) and third order intercept point (IP3) can be calculated [36]–[39]. Finally, the device's linearity performance can be evaluated by adjacent channel power ratio (ACPR) using PL1 and IP3 at the considered bias condition [40].

Pareto optimization is applied using the final version NSGA-III in MATLAB 2018. The basic framework of the

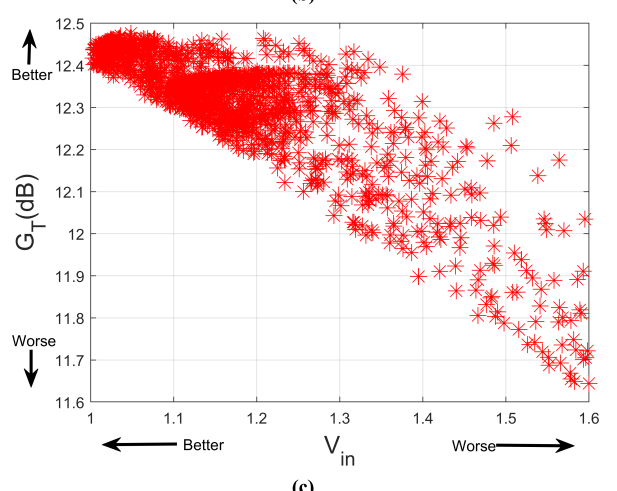
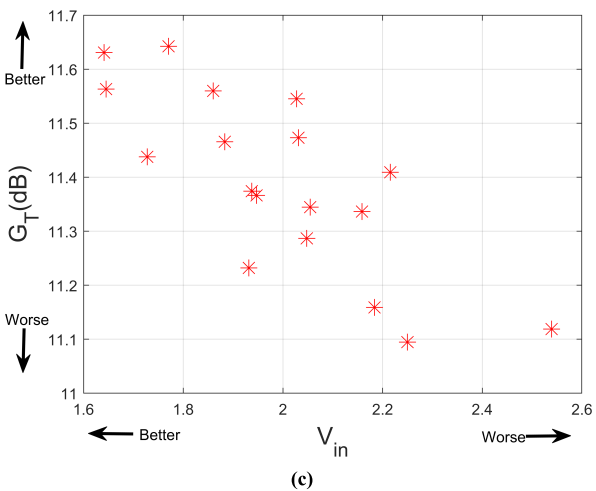
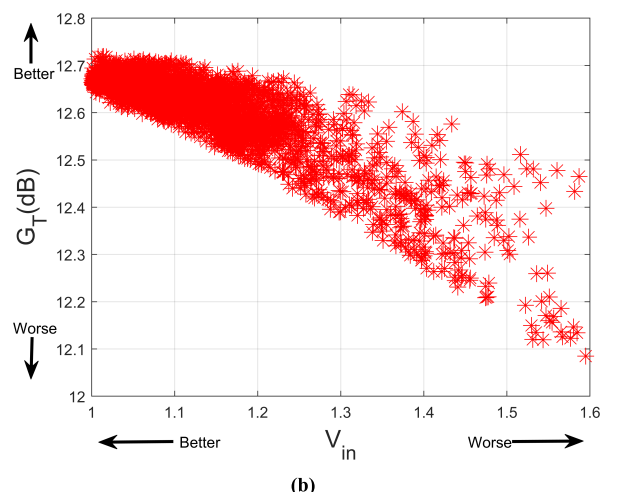
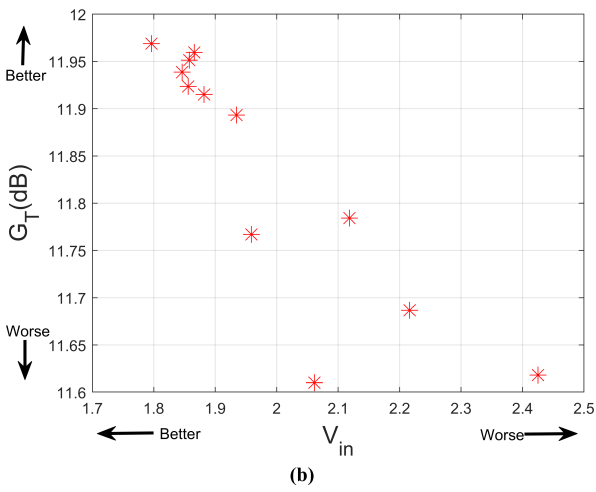
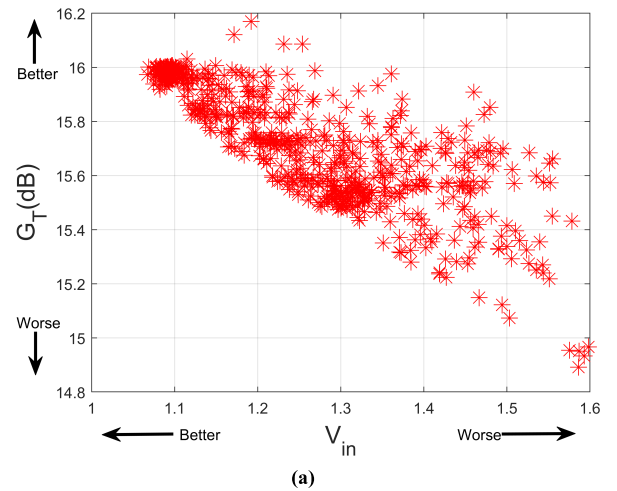
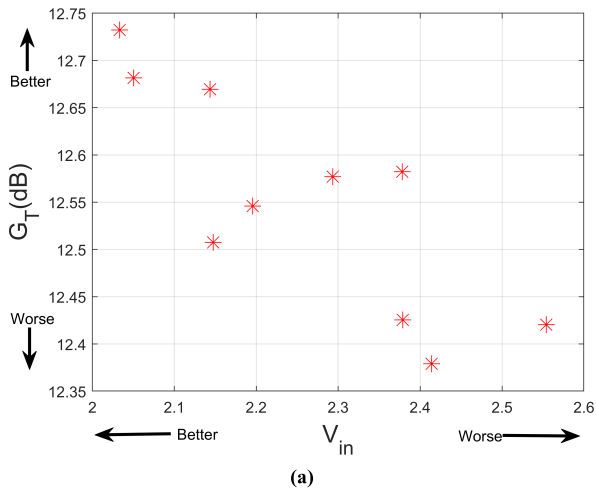


FIGURE 4. Pareto quadruples of (Freq = Fmin, Vinopt, GTmax, Voutreq = 1.2) quadruple for NE3511S02 applying the criterion $V_{in} < 3$ and $V_{out} < V_{outreq} \times 1.03$ and $F < F_{req} \times 1.03$ at bias condition (2V, 10mA): (A) 12GHz, (B) 14GHz, (C) 16GHz.

FIGURE 5. Pareto quadruples of (Freq = 1.3, Vinopt, GTmax, Voutreq = 1.2) quadruple for NE3511S02 applying the criterion $V_{in} < 1.6$ and $V_{out} < V_{outreq} \times 1.03$ and $F < F_{req} \times 1.03$ at bias condition (2V, 10mA): (A) 10GHz, (B) 14GHz, (C) 16GHz.

proposed multi-objective NSGA-III is similar to the original NSGA-II algorithm [33] with the significant changes in its selection operator. But, unlike in NSGA-II, the maintenance of diversity among population members in NSGA-III is aided

by supplying and adaptively updating a number of well-spread reference points with details in [33], [34].

The paper is organized as follows: In the next section, Pareto optimality and flow diagramme of NSGA-III for the transistor POCs will be given briefly. In the third section,

small-signal performance behavior of a LNA transistor will be formulated as a two-port via the system theory and reference points and objectives will also be defined. Then the fourth section gives study case building the POCs using the pre-defined reference points and objective functions in details. Finally, paper ends with the conclusions.

II. PARETO FRONT

A. GENERIC FORMULATION OF MULTI-OBJECTIVE OPTIMIZATION

A minimization multi-objective optimization problem with N objectives is defined as:

$$\text{Minimize } \vec{y} = F(\vec{x}) = [f_1(\vec{x}), f_2(\vec{x}), \dots, f_N(\vec{x})]^T$$

Subject to $g_j(\vec{x}) \leq 0, j = 1, 2, \dots, M$

where $\vec{x} = [x_1, x_2, \dots, x_p]^t \in \Omega$

\vec{y} is the objective vector, the g_j s represent the constraints and \vec{x} is a P-dimensional vector representing the decision variables within a parameter space Ω . The space spanned by the objective vectors is called the objective space. The subspace of the objective vectors that satisfies the constraints is called the feasible space.

B. PARETO OPTIMALITY

A solution \vec{a} is said to be Pareto optimal if and only if there does not exist another solution that dominates it. In other words, solution cannot be improved in one of the objectives without adversely affecting at least one other objective. The corresponding objective vector $F(\vec{a})$ is called a Pareto dominant vector, or non-inferior or non-dominated vector. The set of all Pareto optimal solutions is called the Pareto optimal set. The corresponding objective vectors are said to be on the Pareto fronts. It is generally impossible to come up with an analytical expression of the Pareto front. Figure 1 gives the flow diagram to be followed to obtain POCs of a microwave transistor. In the next section, the objective functions, decision variables and feasibility conditions will be given for multi-objective optimization of the performance characterization of a microwave transistor.

III. REFERENCE BASED MULTI-OBJECTIVE FORMULATION OF THE PERFORMANCE CHARACTERIZATION

A. PERFORMANCE MEASURES

Performance measures of a LNA transistor can be evaluated by the following noise figure F, gain G_T , input V_{in} and output V_{out} VSWRs of a microwave transistor mismatching functions [15], [19], [41], [42]:

$$F = \frac{\text{input}(\frac{\text{signal power}}{\text{noise power}})}{\text{output}(\frac{\text{signal power}}{\text{noise power}})} = F(Z_S) = F_{min} + \frac{R_n |Z_S - Z_{opt}|^2}{|Z_{opt}|^2 R_S} \quad (1)$$

$$G_T(Z_S, Z_L) = \frac{\text{power delivered into the load}}{\text{available source power}}$$

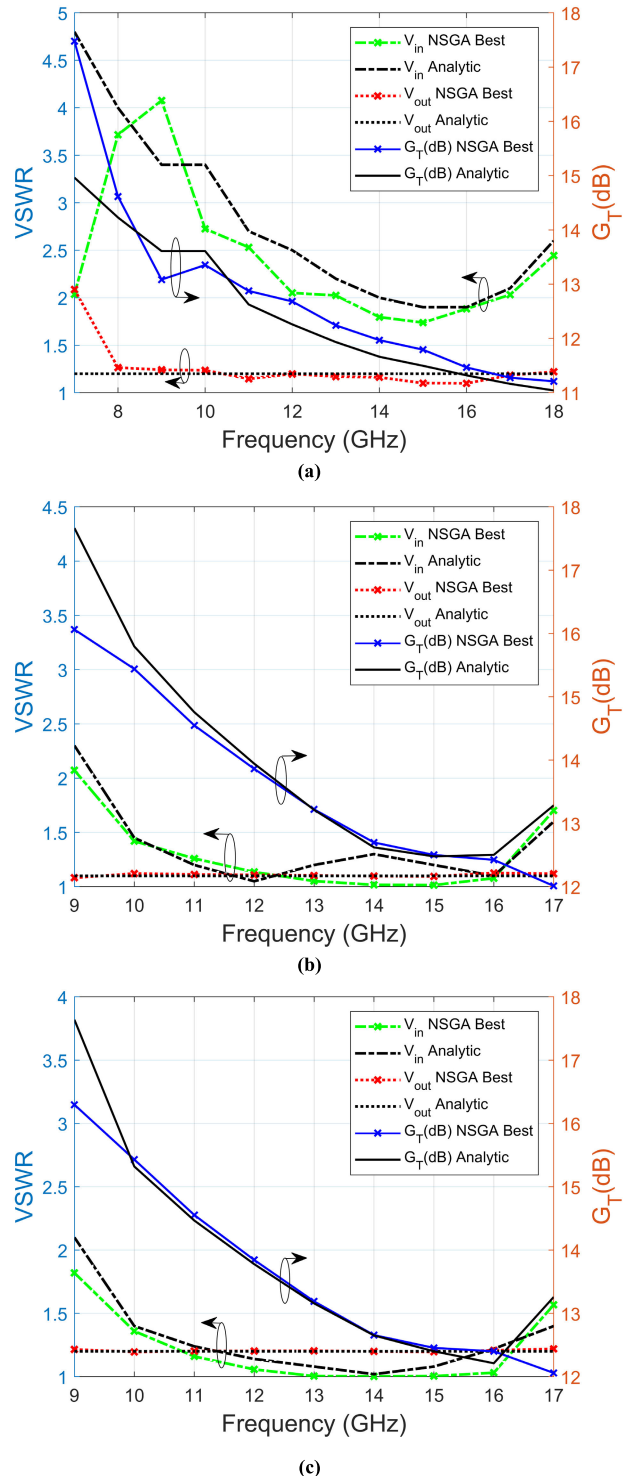


FIGURE 6. Comparison of the analytical and Pareto solutions for the: (A) (Freq = F_{min} , V_{inopt} , G_{Tmax} , $V_{outreq} = 1.2$), (B) (Freq = 1.3, V_{inopt} , G_{Tmax} , $V_{outreq} = 1.1$), (C) (Freq = 1.3, V_{inopt} , G_{Tmax} , $V_{outreq} = 1.2$), quadruple of NE3511S02 at bias condition (2V, 10 mA).

$$G_{AV} = \frac{\text{available output power}}{\text{available input power}} = G_{AV}(Z_S) = \frac{4R_S R_L |z_{21}|^2}{|(z_{11} + Z_S)(z_{22} + Z_L) - z_{12}z_{21}|^2} \quad (2.1)$$

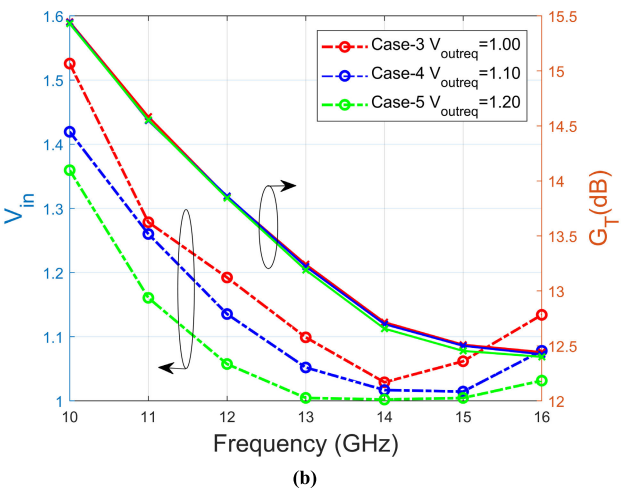
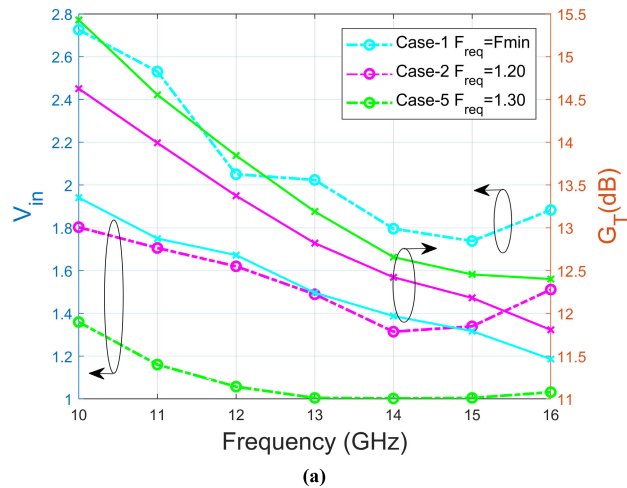


FIGURE 7. Input VSWR (V_{in}) and maximum gain (G_{Tmax}) variations of NE3511S02 applying the criteria $V_{out} < V_{outreq} \times 1.03$ and $F < F_{req} \times 1.03$ at bias condition (2V, 10mA): (A) $V_{outreq} = 1.2$ and taking F_{req} as parameter, (B) $F_{req} = 1.3$ and taking V_{outreq} as parameter.

$$= \frac{|z_{21}|^2 R_S}{|z_{11} + Z_S|^2 R_{out}} \quad (2.2)$$

$$V_{in} = V_{in}(Z_S, Z_L) = \frac{1 + |\rho_{in}|}{1 - |\rho_{in}|}, \quad (3.1)$$

where $|\rho_{in}|^2 = \frac{\text{reflected power at the input port}}{\text{input power}} = \left| \frac{Z_{in} - Z_S^*}{Z_{in} + Z_S} \right|^2 \leq 1$ (3.2)

$$V_{out} = V_{out}(Z_S, Z_L) = \frac{1 + |\rho_{out}|}{1 - |\rho_{out}|}, \quad (4.1)$$

where $|\rho_{out}|^2 = \frac{\text{reflected power at the load}}{\text{load power}} = \left| \frac{Z_{out} - Z_L^*}{Z_{out} + Z_L} \right|^2 \leq 1$ (4.2)

The physical realizability conditions can be given as

$$\text{Re}\{Z_{in}\} = R_{in} = \text{Re}\left\{z_{11} - \frac{z_{12}z_{21}}{z_{22} + Z_L}\right\} > 0 \quad (5)$$

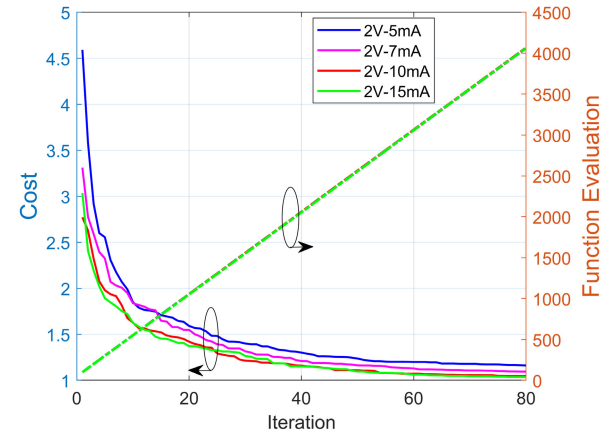


FIGURE 8. Averaged minimum total cost over (10GHz -16GHz) and FEN variations of NE3511S02 for 4 different bias conditions cases of the ($F_{req} = 1.3, V_{inopt}, G_{Tmax}, V_{outreq} = 1.2$) quadruple.

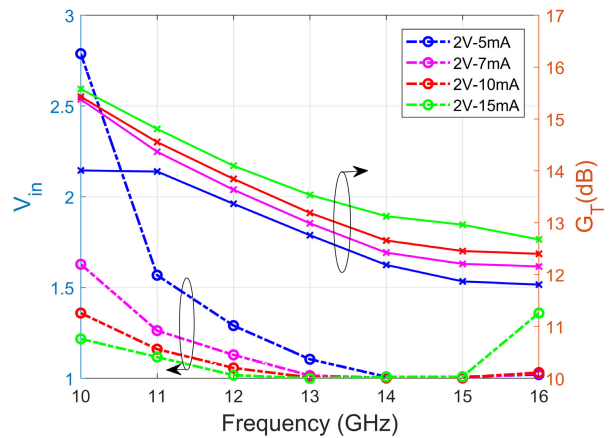


FIGURE 9. V_{in} and Gain G_T variations against frequency of NE3511S02 for ($F_{req} = 1.3, V_{inopt}, G_{Tmax}, V_{outreq} = 1.2$) quadruple and taking 4 bias conditions as parameters.

$$\text{Re}\{Z_{out}\} = R_{out} = \text{Re}\left\{z_{22} - \frac{z_{12}z_{21}}{z_{11} + Z_L}\right\} > 0 \quad (6)$$

$$F \geq F_{min}, \quad V_{in} \geq 1, \quad V_{out} \geq 1, \quad G_{Tmin} \leq G_T \leq G_{Tmax} \quad (7)$$

where the conditions given by (5) and (6) ensure the stable operation of the active device, while the inequalities in (7) guarantees the performance ingredients to remain within the physical limitations of the device.

B. OBJECTIVE FUNCTIONS AND PERFORMANCE QUADRUPLES

Among the measure functions given by (1)-(4), the noise figure F and output V_{out} VSWR are chosen as the reference points, thus 5 performance quadruples are computed as given in Table 1. Accordingly, the following four objective pairs are defined at the selected frequency in the study case:

Objective function 1

$$OF_{11} = \min\{e^{-G_{Ti}/A} + B|F_i - F_{reqi}|\} \quad (8.1)$$

$$OF_{12} = \min\{C|V_{ini}| + D|V_{outi} - V_{outreqi}|\} \quad (8.2)$$

TABLE 4. Pareto optimal and analytical results for the ($f_{req} = 1.3$, V_{inopt} , G_{Tmax} , $V_{outreq} = 1.2$) quadruple of NE3511S02 biased at $V_{DS} = 2V$ and $I_{DS} = 10mA$.

Pareto optimal										Analytical								
f_s GHz	R_s, Ω	X_s, Ω	R_L, Ω	X_L, Ω	V_{in}	V_{out}	F	G_T , dB	Cost	R_s, Ω	X_s, Ω	R_L, Ω	X_L, Ω	V_{in}	V_{out}	F	G_T , dB	Cost
9	10.740	25.781	15.277	24.312	1.818	1.215	1.293	16.317	1.840	5.511	22.235	7.796	30.744	2.100	1.200	1.247	17.638	2.154
10	10.169	14.420	16.161	27.181	1.360	1.196	1.333	15.429	1.397	10.800	16.035	17.150	24.490	1.400	1.200	1.313	15.320	1.513
11	10.050	7.160	16.411	22.724	1.161	1.203	1.328	14.554	1.191	10.860	8.890	17.390	20.560	1.240	1.200	1.305	14.467	1.346
12	10.079	0.709	16.177	18.635	1.058	1.203	1.322	13.845	1.082	11.090	2.155	17.170	16.540	1.140	1.200	1.304	13.779	1.244
13	10.703	-5.351	16.419	13.923	1.005	1.204	1.316	13.190	1.025	11.430	-4.310	17.265	13.380	1.080	1.200	1.301	13.158	1.182
14	11.949	-11.52	16.908	10.357	1.002	1.199	1.315	12.657	1.017	11.870	-10.72	16.790	9.145	1.020	1.200	1.299	12.652	1.119
15	10.921	-16.84	14.226	4.852	1.005	1.197	1.303	12.455	1.011	12.630	-16.26	16.090	5.090	1.080	1.200	1.296	12.401	1.176
16	10.181	-23.42	12.188	0.856	1.032	1.208	1.330	12.401	1.069	14.450	-22.01	15.975	1.125	1.220	1.200	1.310	12.212	1.331
17	19.169	-26.49	17.840	-4.132	1.567	1.214	1.319	12.063	1.599	7.012	-31.36	6.537	-2.553	1.400	1.200	1.360	13.259	1.461

Objective function 2

$$OF_{21} = \min\{e^{-G_T/A} + B|V_{outi} - V_{outreqi}|\} \quad (9.1)$$

$$OF_{22} = \min\{C|F_i - F_{reqi}| + D|V_{ini}|\} \quad (9.2)$$

Objective function 3

$$OF_{31} = \min\{e^{-G_T/A} + +B|V_{ini}| + C|V_{outi} - V_{outreqi}|\} \quad (10.1)$$

$$OF_{32} = \min\{D|F_i - F_{reqi}|\} \quad (10.2)$$

Objective function 4

$$OF_{41} = \min\{e^{-G_T/A}\} \quad (11.1)$$

$$OF_{42} = \min\{B|F_i - F_{reqi}| + C|V_{ini}| + D|V_{outi} - V_{outreqi}|\} \quad (11.2)$$

where $F_{reqi} \geq F_{mini}$ and $V_{outreqi} \geq 1$, $i = 1, 2, \dots, 5$ are supplied as the reference points which take the values given in Table 1 as the pre-defined 5 performance quadruples. Each objective function pair is used to form a single cost function as follows:

$$\text{cost} = OF_{i1} + OF_{i2}, i = 1, 2, \dots, 4 \quad (12)$$

Since independent analysis must be made for each pre-defined performance quadruple at each sample frequency, therefore the objective function pair to be used in the related Pareto optimization process must be determined separately as the one function pair having the minimum averaged cost taken over the 10 runs among the $(OF_{i1} + OF_{i2})$ $i = 1, \dots, 4$ in (8.1) - (11.2).

In this optimization process decision variables are the real (R_s, R_L) and imaginary (X_s, X_L) parts of the source Z_s and load Z_L impedances, respectively. All the weighting

coefficients are taken as unity throughout all the cases since all the requirements have been considered as having equal significance.

In the optimization process, we work out with the feasible solutions of the performance measure equations given by (1) - (4) taken place within the unconditionally stable working area (USWA) defined by the eqs. (5) - (7), therefore finite gains are interested with the feasible passive terminations having $R_s > 10\Omega$ and $R_L > 10\Omega$. Besides, since GA is a randomly initialized algorithm at each run of the algorithm different solution can be obtained. Thus, for a precise performance evaluation of the Pareto front belonging to each performance ($f_{req}, V_{inopt}, G_{Tmax}, V_{outreq}$) quadruple at each sample frequency, at least 10 different runs of NSGA-III are required to obtain the best, worst solution values with using an objective function pair in (8.1) - (11.2).

In the next section, a study case will be presented choosing a LNA transistor NE3511S02 as a test vehicle whose Pareto fronts will be computed at the bias condition $V_{DS} = 2V$ and $I_{DS} = 10mA$ for the frequency between 9GHz - 18GHz.

IV. STUDY CASE

A. OBJECTIVE FUNCTION PAIR

In order to obtain the Pareto fronts, firstly, the objective function pair with the minimum averaged cost must be determined for each pre-defined performance quadruple at each sample frequency. For this purpose, the NSGA-III is implemented to each pre-defined performance quadruple at table 1 at each sample frequency using each the objective function pair given by (8.1) - (11.2) using the default parameters of maximum iteration = 50, population = 50, crossover percentage = 0.5 and mutation = 0.5. Thus, 25000 results are obtained to

TABLE 5. The best and worst cost values of 10 different runs for bias domains.

Power	Domain	Cost State	Cost (10 GHz)	Cost (11 GHz)	Cost (12 GHz)	Cost (13 GHz)	Cost (14 GHz)	Cost (15 GHz)	Cost (16 GHz)	Cost (Total)
10mW	2V-5mA	Best	2.889	1.600	1.330	1.134	1.023	1.025	1.057	10.057
		Worst	4.176	2.338	1.359	2.095	1.562	1.187	1.255	13.972
14mW	2V-7mA	Best	1.664	1.299	1.167	1.049	1.010	1.007	1.047	8.242
		Worst	3.953	3.152	1.880	1.177	1.115	1.228	1.388	13.894
20mW	2V-10mA	Best	1.397	1.191	1.082	1.025	1.017	1.011	1.069	7.793
		Worst	1.819	1.235	1.399	1.301	1.279	1.153	1.403	9.589
30mW	2V-15mA	Best	1.247	1.136	1.030	1.023	1.031	1.038	1.396	7.902
		Worst	1.758	1.776	1.114	1.535	1.186	1.328	1.811	10.508

TABLE 6. Best, worst and mean cost results obtained from 10 different runs for NSGA-III of (Freq = 1.3, V_{inopt} , G_{Tmax} , $V_{outreq} = 1.2$) quadruple at $V_{DS} = 2V$ and $I_{DS} = 5mA$.

f, GHz	V_{in} Best Cost	V_{in} Worst Cost	V_{in} Mean Cost	V_{out} Best Cost	V_{out} Worst Cost	V_{out} Mean Cost	F Best Cost	F Worst Cost	F Mean Cost	G_T , dB Best Cost	G_T , dB Worst Cost	G_T , dB Mean Cost
10	2.788	3.923	2.427	1.102	1.264	1.276	1.302	1.112	1.299	14.007	11.867	14.034
11	1.568	2.077	2.320	1.199	1.356	1.227	1.331	1.195	1.258	13.987	13.260	13.164
12	1.291	1.263	1.576	1.176	1.159	1.189	1.316	1.354	1.300	13.365	13.412	13.087
13	1.105	2.010	1.404	1.203	1.192	1.148	1.326	1.223	1.307	12.760	12.199	12.607
14	1.009	1.524	1.103	1.193	1.191	1.194	1.308	1.329	1.319	12.187	11.780	12.125
15	1.008	1.163	1.050	1.198	1.195	1.198	1.315	1.319	1.315	11.869	11.781	11.848
16	1.021	1.155	1.079	1.196	1.123	1.188	1.332	1.324	1.321	11.806	11.821	11.784

TABLE 7. Best, worst and mean cost results obtained from 10 different runs for NSGA-III of (Freq = 1.3, V_{inopt} , G_{Tmax} , $V_{outreq} = 1.2$) quadruple at $V_{DS} = 2V$ and $I_{DS} = 7mA$.

f, GHz	V_{in} Best Cost	V_{in} Worst Cost	V_{in} Mean Cost	V_{out} Best Cost	V_{out} Worst Cost	V_{out} Mean Cost	F Best Cost	F Worst Cost	F Mean Cost	G_T , dB Best Cost	G_T , dB Worst Cost	G_T , dB Mean Cost
10	1.628	3.658	2.126	1.202	1.038	1.158	1.333	1.167	1.294	15.379	12.696	14.590
11	1.263	2.958	1.784	1.208	1.084	1.157	1.328	1.222	1.286	14.367	12.558	13.768
12	1.130	1.857	1.287	1.187	1.176	1.168	1.325	1.300	1.319	13.636	12.843	13.499
13	1.015	1.110	1.063	1.202	1.236	1.198	1.331	1.331	1.326	12.989	12.904	12.967
14	1.003	1.091	1.025	1.200	1.208	1.200	1.307	1.316	1.312	12.424	12.370	12.414
15	1.002	1.202	1.051	1.200	1.205	1.202	1.305	1.321	1.308	12.207	12.057	12.182
16	1.027	1.344	1.093	1.198	1.182	1.197	1.318	1.327	1.322	12.157	11.941	12.108

be averaged for each objective function pair at each sample frequency. Objective function pair $OF_{41} + OF_{42}$ (11.1) - (11.2) is resulted for the objective function pair to be used for each performance quadruple at each sample frequency that can be seen from the typical convergence variations of all the possible cost functions given in Figures 2A, 2B and 2C.

B. OPTIMAL ALGORITHM PARAMETER SET SELECTION

The default parameters of the NSGA-III algorithm are given as maximum iteration = 50, population = 50, crossover percentage (P_c) = 0.5 and mutation (P_m) = 0.5. In this study case, maximum number of iteration = 80, population = 50, crossover percentage = 0.3 and mutation = 0.8 are used as the

TABLE 8. Monte Carlo analysis results for ($F_{req} = 1.3, V_{inopt}, G_{Tmax}, V_{outreq} = 1.2$) quadruple at $V_{DS} = 2V$ and $I_{DS} = 7mA$.

f, GHz	V_{in} (Target)	V_{in} (Worst)	V_{in} (Mean)	V_{out} (Target)	V_{out} (Worst)	V_{out} (Mean)	F (Target)	F (Worst)	F (Mean)	G_T, dB (Target)	G_T, dB (Worst)	G_T, dB (Mean)
10	1.628	1.798	1.632	1.202	1.093	1.208	1.333	1.330	1.334	15.379	15.326	15.375
11	1.263	1.361	1.265	1.208	1.117	1.211	1.328	1.338	1.328	14.367	14.365	14.365
12	1.130	1.215	1.131	1.187	1.101	1.189	1.325	1.330	1.325	13.636	13.637	13.635
13	1.015	1.086	1.030	1.202	1.120	1.204	1.331	1.342	1.331	12.989	12.998	12.987
14	1.003	1.083	1.029	1.200	1.292	1.202	1.307	1.308	1.307	12.424	12.399	12.422
15	1.002	1.100	1.037	1.200	1.109	1.202	1.305	1.295	1.305	12.207	12.212	12.205
16	1.027	1.106	1.057	1.198	1.305	1.202	1.318	1.330	1.318	12.157	12.128	12.154

TABLE 9. Comparison between the computed values presented in Table 7 and the circuit simulator results.

f, GHz	R_s, Ω	X_s, Ω	R_L, Ω	X_L, Ω	V_{in} (Com.)	V_{in} (Sim.)	V_{out} (Com.)	V_{out} (Sim.)	F (Com.)	F (Sim.)	G_T, dB (Com.)	G_T, dB (Sim.)
10	10.131	16.217	14.494	23.451	1.628	1.470	1.202	1.117	1.333	1.184	15.379	15.389
11	10.039	8.669	15.736	20.463	1.263	1.218	1.208	1.161	1.328	1.189	14.367	14.534
12	10.033	1.671	15.380	16.494	1.130	1.090	1.187	1.180	1.325	1.194	13.636	13.839
13	10.065	-5.279	15.397	14.380	1.015	1.030	1.202	1.170	1.331	1.201	12.989	13.214
14	11.053	-10.592	15.907	8.438	1.003	1.036	1.200	1.210	1.307	1.183	12.424	12.660
15	10.786	-16.767	14.316	4.524	1.002	1.021	1.200	1.223	1.305	1.197	12.207	12.447
16	10.016	-23.624	12.040	0.489	1.027	1.015	1.198	1.226	1.318	1.231	12.157	12.403

optimum parameter set which is found from the Case-5 corresponding to the ($F_{req} = 1.3, V_{inopt}, G_{Tmax}, V_{outreq} = 1.2$) quadruple at the operation condition of 2V, 10mA, 12GHz. Comparison between cost and function evaluation number (FEN) variations for the default and optimum parameter sets of NSGA-III algorithm are given in Figures 3A and 3B.

C. PARETO QUADRUPLES

Pareto ($F_{req}, V_{inopt}, G_{Tmax}, V_{outreq}$) quadruples of the transistor NE3511S02 are obtained for five (F_{req}, V_{outreq}) pairs which are ($F_{min}, 1.2$), (1.1, 1.2), (1.3, 1), (1.3, 1.1) and (1.3, 1.2) as given in Table 1 for bias condition of 2V, 10mA. 10×4050 Pareto optimal solutions are resulted from the 10 different runs of NSGA-III using the objective function (OF_{41}, OF_{42}) pair at each sample frequency forming the Pareto front. The required Pareto ($F_{req}, V_{inopt}, G_{Tmax}, V_{outreq}$) quadruples at each sample frequency are generated analyzing these 10×4050 data based upon the required criterion. Thus typical Pareto quadruples of NE3511S02 can be seen from Figures 4A, 4B and 4C and Figures 5A, 5B and 5C, taken place on the $V_{in} - G_T$ plane at 10GHz, 12GHz, 14GHz and 16GHz, belonging to the ($F_{req} = F_{min}, V_{inopt}, G_{Tmax}, V_{outreq} = 1.2$) and ($F_{req} = 1.3, V_{inopt}, G_{Tmax}, V_{outreq} = 1.2$) quadruples, respectively. Pareto ($F_{req}, V_{inopt}, G_{Tmax}, V_{outreq}$)

quadruples in Figures 4A, 4B and 4C and Figures 5A, 5B and 5C guarantee $V_{in} < 3$ or $V_{in} < 1.6$ and $V_{out} < V_{outreq} \times 1.03$ and $F < F_{req} \times 1.03$, respectively within the 10×4050 Pareto optimal solutions as pointed out in the related figures. It should be noted that, the selected performance criterions might bring limitations to the operation band. Thus, in order to extend the operation band, one might consider to loosen the strict conditions of Pareto ($F_{req}, V_{inopt}, G_{Tmax}, V_{outreq}$) quadruples at expense of the increased cost function value for extending the operation bandwidth.

D. PARETO OPTIMAL CHARACTERISTICS

Pareto optimal characteristics (POCs) are built up in the ($V_{SWR}/G_T - f$) plane using the Pareto quadruples having the minimum cost ($OF_{41} + OF_{42}$), in the other words the best quadruples at each operation frequency. For the purpose of comparison Pareto optimal and the corresponding analytical characteristics [15], the quadruples ($F_{req} = F_{min}, V_{inopt}, G_{Tmax}, V_{outreq} = 1.2$), ($F_{req} = 1.3, V_{inopt}, G_{Tmax}, V_{outreq} = 1.1$) and ($F_{req} = 1.3, V_{inopt}, G_{Tmax}, V_{outreq} = 1.2$) within the 7GHz - 18GHz band are combined as graphics in Figures 6A, 6B and 6C and numerical in Table 2-4, respectively. Here it should be noted that the analytical solution leads to only one solution, whereas Pareto optimization finds out

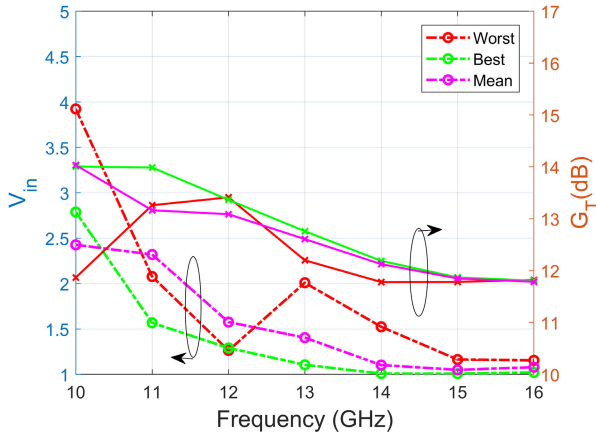


FIGURE 10. Best, worst and mean Pareto characteristics of 10 different runs for ($F_{req} = 1.3, V_{inopt}, G_{Tmax}, V_{outreq} = 1.2$) quadruple at bias condition (2V, 5mA).

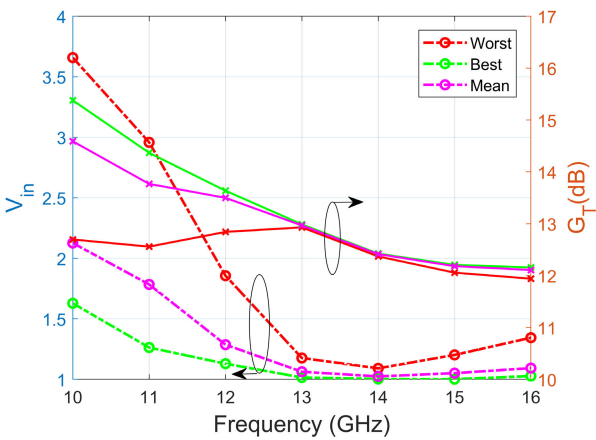


FIGURE 11. Best, worst and mean Pareto characteristics of 10 different runs for ($F_{req} = 1.3, V_{inopt}, G_{Tmax}, V_{outreq} = 1.2$) quadruple at bias condition (2V, 7mA).

the solution set around. Here, one can infer that diversity property of NSGA-III brings out superior characteristics of the transistor’s potential performance that cannot be obtained easily from the analytical work. Thus, Figures 7A and 7B give comparative (V_{in} / G_T) – f variations built up within 10GHz–16GHz.

E. OPTIMUM BIAS CONDITION

The optimum bias condition will be determined within 10GHz–16GHz band for the considered performance quadruple. For this purpose, firstly the bias conditions (V_{DS}, I_{DS}) are chosen satisfying $I_{DS} \leq I_{max}$ and $V_{DS} \times I_{DS} \leq P_{max}$ where I_{max} and P_{max} are pre-determined. The criterions can be selected to take sum of the best (13) or worst (14) costs chosen among 10 runs at each operation frequency:

$$\text{total cost} = \sum_{j=10GHz}^{16GHz} \min\{NOR_i\{\min(OF_{41j} + OF_{42j})\}\} \tag{13}$$

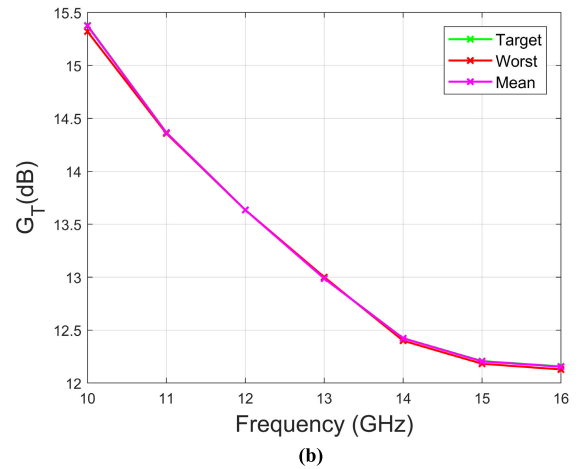
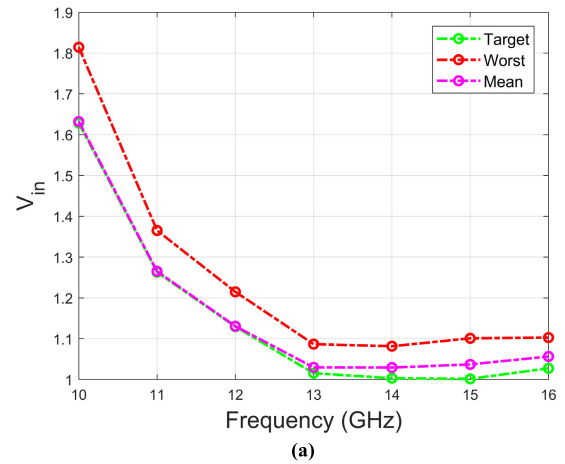


FIGURE 12. Target, worst and mean: (A) V_{inopt} (B) G_T variations for ($F_{req} = 1.3, V_{inopt}, G_{Tmax}, V_{outreq} = 1.2$) quadruple of NE3511S02 resulted from Monte Carlo analysis at bias condition (2V, 7mA).

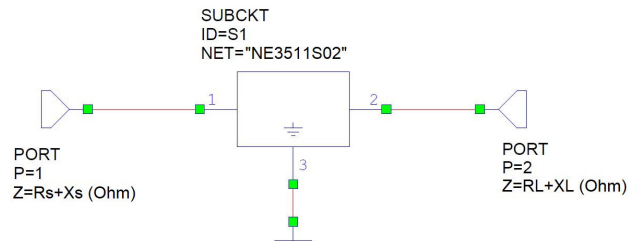


FIGURE 13. AWR schematic of the LNA model.

$$\text{total cost} = \sum_{j=10GHz}^{16GHz} \max\{NOR_i\{\min(OF_{41j} + OF_{42j})\}\} \tag{14}$$

where, $i: 1, 2, \dots, 10$, NOR: Number of run.

The power-based analysis for 10, 14, 20 and 30mW are given in Table 5 for the ($F_{req} = 1.3, V_{inopt}, G_{Tmax}, V_{outreq} = 1.2$) quadruple whose cost and FEN variations with iteration are shown for the considered bias conditions in Figure 8. Besides (V_{in} / G_T) – f variations for the ($F_{req} = 1.3, V_{inopt}, G_{Tmax}, V_{outreq} = 1.2$) quadruple are given for all the considered bias conditions in Figure 9. Furthermore, the best

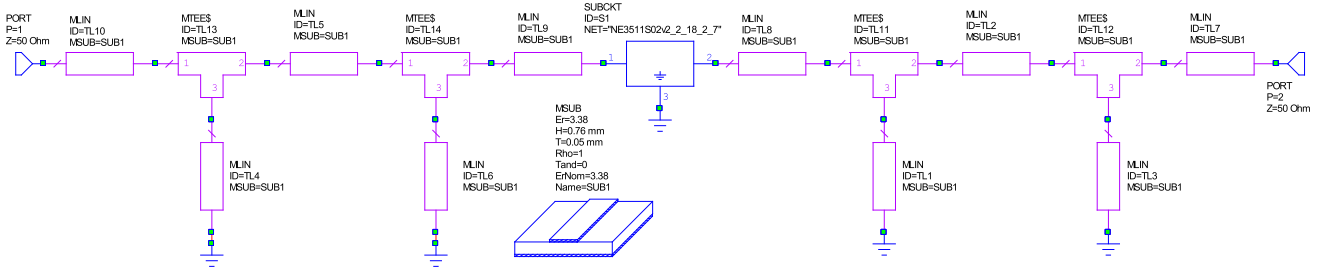


FIGURE 14. AWR schematic of the LNA model.

TABLE 10. Pareto optimal and network matching results for the ($F_{req} = 1.3$, V_{inopt} , G_{Tmax} , $V_{outreq} = 1.2$) quadruple of NE3511S02 biased at $V_{DS} = 2V$ and $I_{DS} = 7mA$.

Pareto optimal							Network Matching AWR									
f, GHz	R_S, Ω	X_S, Ω	R_L, Ω	X_L, Ω	V_{in}	V_{out}	F	G_T, dB	R_S, Ω	X_S, Ω	R_L, Ω	X_L, Ω	V_{in}	V_{out}	F	G_T, dB
10	10.131	16.217	14.494	23.451	1.628	1.202	1.333	15.379	8.131	10.980	14.494	22.770	1.900	1.400	1.420	15.450
11	10.039	8.669	15.736	20.463	1.263	1.208	1.328	14.367	10.560	5.500	15.736	23.300	1.300	1.250	1.230	14.190
12	10.033	1.671	15.380	16.494	1.130	1.187	1.325	13.636	12.090	2.870	15.380	19.200	1.300	1.200	1.170	13.460
13	10.065	-5.279	15.397	14.380	1.015	1.202	1.331	12.989	11.830	-1.220	15.397	14.660	1.500	1.300	1.160	12.720
14	11.053	-10.590	15.907	8.438	1.003	1.200	1.307	12.424	8.870	-11.050	15.907	10.280	1.170	1.170	1.270	12.330

and worst cost values can be seen in Table 5 for the chosen conditions. Moreover, the worst, mean and best cost values of the ($F_{req} = 1.3$, V_{inopt} , G_{Tmax} , $V_{outreq} = 1.2$) quadruple at bias conditions (2V, 5mA and 2V, 7mA) can be followed at each operation frequency as numerical and graphics from tables in Tables 6-7 and Figures 10-11, respectively.

F. MONTE CARLO ANALYSIS

In this work, briefly using NSGA-III, we have determined compatible ($F_{req} \geq F_{min}$, V_{inopt} , G_{Tmax} , $V_{outreq} \geq 1$) quadruples with their (Z_S, Z_L) terminations with $Re\{Z_S\} > 0$ and $Re\{Z_L\} > 0$ over the operational bandwidth of a LNA transistor as functions of the device’s operation parameters (V_{DS} , I_{DS} , f) where V_{DS} , I_{DS} stand for bias voltage and current respectively; f is the operation frequency. As reference to network theory, realizability of the passive (Z_S, Z_L) termination pair is based upon the fundamental theorem of Darlington which expresses that any impedance function $Z(\omega) = R(\omega) + jX(\omega)$ with $R(\omega) > 0$ within the operational bandwidth can be realized by a (L-C) two-port terminated by 1Ω . In fact, we have a work [43] using Darlington theorem on realization of the potential performance terminations of a transistor. However, these realizations are ideal, in practical situations reactive components L, C have losses which entail detrimental effects on the performance of the network, but this situation is inevitable. These detrimental effects are accounted by randomly changing real and imaginary parts of both the source and load terminations via Monte Carlo analysis.

Monte Carlo analysis is applied for ($F_{req} = 1.3$, V_{inopt} , G_{Tmax} , $V_{outreq} = 1.2$) quadruple for the bias condition (2V, 7mA). In this analysis, each of real (R_S, X_S, R_L, X_L) variables is changed randomly in the range of ($\pm 5\%$) about their optimal values at each sample frequency, thus total 10000 random source and load termination couples are generated for each sample frequency, then the worst and mean values are determined after the performance analysis has been completed for each randomly generated source and load couple. Results of Monte Carlo analysis can be followed as numerical and graphics from Table 8 and Figures 12A and 12B respectively. From this analysis, it can be inferred that the Z_S and Z_L terminations are weakly sensitive to the tolerances for ($F_{req} = 1.3$, V_{inopt} , G_{Tmax} , $V_{outreq} = 1.2$) quadruple. Furthermore, a circuit simulation is also completed giving the optimal Z_S and Z_L termination couples to the AWR simulator (Figure 13), the resulted performance ingredients are given in Table 9 as compared with the Pareto optimal values.

G. TYPICAL APPLICATIONS

In [43], L-C front-end and back-end matching circuits of a LNA transistor are designed to provide its source Z_S and load Z_L terminations of its required compatible ($F_{req} \geq F_{min}$, V_{inreq} , G_{Tmax}) triplet over the predetermined bandwidth B between f_{min} and f_{max} operation frequencies.

Besides we carried out design optimization process of a microstrip LNA between 10GHz - 14GHz for NE3511S02 at its optimal bias condition $V_{DS} = 2V$ and $I_{DS} = 7mA$. In this design optimization process, Pareto quadruple ($F_{req} = 1.3$,

TABLE 11. Widths and lengths value of the matching networks in (mm).

$W_1=0.85$	$L_1=0.1$	$W_6=1.6$	$L_6=7.1$
$W_2=3.2$	$L_2=7.5$	$W_7=3.6$	$L_7=4.0$
$W_3=6.3$	$L_3=4.2$	$W_8=1.9$	$L_8=0.1$
$W_4=0.4$	$L_4=4.3$	$W_9=11.9$	$L_9=0.6$
$W_5=11.1$	$L_5=1.8$	$W_{10}=6.0$	$L_{10}=3.0$

V_{inopt} , G_{Tmax} , $V_{outreq} = 1.2$) and the associated source Z_S and load Z_L , are used as the design target and the resulted performance and element values are listed in Table 10 and 11, respectively. Furthermore, the circuit scheme is given in Figure 14.

V. CONCLUSION

In this work, for the first time in the literature, a microwave small-signal transistor's potential performance is formulated as a multi-objective optimization problem and expressed in terms of the Pareto optimal solutions and trade-off relations that cannot be obtained with either analytical or single-objective optimization. Briefly, all these Pareto optimal solutions cover all the capability of the transistor's performance itself. Physical features of these solutions can also be investigated using the analytical work in [15]. Thus, FDTS ingredient of the LNA design optimization problem can be built up completely without any expert knowledge, obtaining all the set of acceptable non-dominated solutions with together with their trade-off relations within the device operation (V_{DS} , I_{DS} , f) domain. For this purpose, user-preference based NSGA-III is used, where the noise $F_{req} \geq F_{min}$ and output mismatching $V_{outreq} \geq 1$ are chosen as the reference points. NSGA-III uses the framework of NSGA-II, but works with a set of supplied or pre-defined reference points and demonstrate its efficacy in solving two-objective to 15 objective optimization problems. Furthermore, analyses of "Optimum Bias Condition" and "Detrimental effects of the Termination Tolerances" are also completed.

Moreover, a typical LNA transistor NE3511S02 is considered as a study case and its potential performance and trade-off relations are derived for its operation between 10GHz and 16GHz at $V_{DS} = 2V$ and $I_{DS} = 5, 7, 10$ and $15mA$. Thus, all the ($F_{req} \geq F_{min}$, $V_{in} \geq 1$, $G_{Tmin} \leq G_T \leq G_{Tmax}$) quadruples can be obtained with their feasible (Source Z_S , Load Z_L) termination pairs within the device operation domain of (V_{DS} , I_{DS} , f) so that all the possible LNA designs can be overviewed.

It can be concluded that any challenging LNA design can be achieved using this work combining with the novel algorithms and technology.

REFERENCES

- [1] F. Güneş, H. Torpi, and F. Gürgeç, "Multidimensional signal-noise neural network model," *IEE Proc. Circuits, Devices Syst.*, vol. 145, no. 2, pp. 111–117, 1998, doi: [10.1049/ip-cds:19981712](https://doi.org/10.1049/ip-cds:19981712).
- [2] F. F. Güneş, N. Türker and F. Gürgeç, "Signal-noise support vector model of a microwave transistor," *Int. J. RF Microw. Comput.-Aided Eng.*, vol. 17, no. 4, pp. 404–415, Jul. 2007.
- [3] F. Güneş, P. Mahouti, S. Demirel, M. A. Belen, and A. Uluslu, "Cost-effective GRNN-based modeling of microwave transistors with a reduced number of measurements," *Int. J. Numer. Model., Electron. Netw., Devices Fields*, vol. 30, nos. 3–4, Aug. 2015, Art. no. 2089, doi: [10.1002/jnm.2089](https://doi.org/10.1002/jnm.2089).
- [4] F. Güneş, M. A. Belen, P. Mahouti, and S. Demirel, "Signal and noise modelling of microwave transistors using characteristic support vector-based sparse regression," *Radioengineering*, vol. 25, no. 3, Sep. 2016, doi: [10.13164/re.2016.0490](https://doi.org/10.13164/re.2016.0490).
- [5] D. Dousset, A. Issaoun, F. M. Ghannouchi, and A. B. Kouki, "Wideband closed-form expressions for direct extraction of HBT small-signal parameters for all amplifier bias classes," *IEE Proc. Circuits, Devices Syst.*, vol. 152, no. 5, p. 441, 2005, doi: [10.1049/ip-cds:20045077](https://doi.org/10.1049/ip-cds:20045077).
- [6] V. J. Vijayakrishna, S. Vaishnav, N. DasGupta, and A. DasGupta, "Unified analytical model of HEMTs for analogue and digital applications," *IEE Proc. Circuits, Devices Syst.*, vol. 152, no. 5, p. 425, 2005, doi: [10.1049/ip-cds:20045087](https://doi.org/10.1049/ip-cds:20045087).
- [7] N. Seoane and A. J. García-Loureiro, "Study of parallel numerical methods for semiconductor device simulation," *Int. J. Numer. Model., Electron. Netw., Devices Fields*, vol. 19, no. 1, pp. 15–32, 2005, doi: [10.1002/jnm.596](https://doi.org/10.1002/jnm.596).
- [8] A. Caddemi, G. Crupi, and A. Macchiarella, "On wafer-scaled GaAs HEMTs: Direct and robust small signal modeling up to 50 GHz," *Microw. Opt. Technol. Lett.*, vol. 51, no. 8, pp. 1958–1963, Aug. 2009, doi: [10.1002/mop.24492](https://doi.org/10.1002/mop.24492).
- [9] M. Muhamad, N. Soin, H. Ramiah, N. M. Noh, and C. W. Keat, "On-wafer scattering parameter characterization of differential four-port networks LNA using two-port vector network analyzer," in *Proc. IEEE Int. Conf. Semicond. Electron. (ICSE)*, Aug. 2014, pp. 339–342, doi: [10.1109/SMELEC.2014.6920867](https://doi.org/10.1109/SMELEC.2014.6920867).
- [10] J. Randa and D. K. Walker, "On-wafer measurement of transistor noise parameters at NIST," *IEEE Trans. Instrum. Meas.*, vol. 56, no. 2, pp. 551–554, Apr. 2007, doi: [10.1109/TIM.2007.891145](https://doi.org/10.1109/TIM.2007.891145).
- [11] A. Wu, C. Li, J. Sun, Y. Wang, and C. Liu, "Development of a verification technique for on-wafer noise figure measurement systems," in *Proc. 90th ARFTG Microw. Meas. Symp. (ARFTG)*, Nov. 2017, pp. 1–4, doi: [10.1109/ARFTG.2017.8255878](https://doi.org/10.1109/ARFTG.2017.8255878).
- [12] F. Gunes, M. Gunes, and M. Fidan, "Performance characterization of a microwave transistor," *IEE Proc. Circuits Devices Syst.*, vol. 141, pp. 337–344, Oct. 1994.
- [13] F. Güneş and B. A. Çetiner, "Smith chart formulation of performance characterisation for a microwave transistor," *IEE Proc. Circuits, Devices Syst.*, vol. 145, no. 6, pp. 419–428, 1998.
- [14] S. Demirel and F. Güneş, "Performance characterisation of a microwave transistor for the maximum output power and the required noise," *IET Circuits, Devices Syst.*, vol. 7, no. 1, pp. 9–20, Jan. 2013.
- [15] F. Güneş and S. Demirel, "Performance characterization of a microwave transistor subject to the noise and matching requirements," *Int. J. Circuit Theory Appl.*, vol. 44, no. 5, pp. 1012–1028, Aug. 2015, doi: [10.1002/cta.2120](https://doi.org/10.1002/cta.2120).
- [16] F. Güneş, U. Özkaya, and S. Demirel, "Particle swarm intelligence applied to determination of the feasible design target for a low-noise amplifier," *Microw. Opt. Technol. Lett.*, vol. 51, no. 5, pp. 1214–1218, May 2009.
- [17] F. Güneş, S. Demirel, and P. Mahouti, "A simple and efficient honey bee mating optimization approach to performance characterization of a microwave transistor for the maximum power delivery and required noise," *Int. J. Numer. Model., Electron. Netw., Devices Fields*, vol. 29, no. 1, pp. 4–20, Jan. 2015, doi: [10.1002/jnm.2041](https://doi.org/10.1002/jnm.2041).
- [18] M. A. Belen, M. Alic, A. Çor, and F. Güneş, "Performance characterization of a microwave transistor using firefly algorithm," in *Proc. Symp. Elect.-Electron. Comput. Eng. (ELECO, (in Turkish))*, Bursa, Turkey, Nov. 2014, pp. 491–493.
- [19] F. Güneş, M. A. Belen, and P. Mahouti, "Competitive evolutionary algorithms for building performance database of a microwave transistor," *Int. J. Circuit Theory Appl.*, vol. 46, no. 2, pp. 244–258, Aug. 2017, doi: [10.1002/cta.2386](https://doi.org/10.1002/cta.2386).

- [20] N. M. Moraes, U. H. Bezerra, J. L. Moya Rodríguez, M. H. R. Nascimento, and J. C. Leite, "A new approach to economic-emission load dispatch using NSGA II. Case study," *Int. Trans. Electr. Energy Syst.*, vol. 28, no. 11, May 2018, Art. no. e2626, doi: [10.1002/etep.2626](https://doi.org/10.1002/etep.2626).
- [21] S. Luo, C. Liu, L. Zhang, and Y. Fan, "An improved nondominated sorting genetic algorithm-II for multi-objective flexible job-shop scheduling problem," in *Proc. IEEE Symp. Ser. Comput. Intell. (SSCI)*, Nov. 2018, pp. 569–577, doi: [10.1109/SSCI.2018.8628824](https://doi.org/10.1109/SSCI.2018.8628824).
- [22] S. Khebbache, M. Hadji, and D. Zeglache, "A multi-objective non-dominated sorting genetic algorithm for VNF chains placement," in *Proc. 15th IEEE Annu. Consum. Commun. Netw. Conf. (CCNC)*, Jan. 2018, pp. 1–4, doi: [10.1109/CCNC.2018.8319250](https://doi.org/10.1109/CCNC.2018.8319250).
- [23] F. Jauhari, W. F. Mahmudy, and A. Basuki, "Multi-objective optimization for proportional tuition fees assessment using non-dominated sorting genetic algorithm II (NSGA II)," in *Proc. Int. Conf. Sustain. Inf. Eng. Technol. (SIET)*, Nov. 2018, pp. 292–297, doi: [10.1109/SIET.2018.8693182](https://doi.org/10.1109/SIET.2018.8693182).
- [24] A. M. Eldurssi and R. M. O'Connell, "A fast nondominated sorting guided genetic algorithm for multi-objective power distribution system reconfiguration problem," *IEEE Trans. Power Syst.*, vol. 30, no. 2, pp. 593–601, Mar. 2015, doi: [10.1109/TPWRS.2014.2332953](https://doi.org/10.1109/TPWRS.2014.2332953).
- [25] S. K. Goudos and J. N. Sahalos, "Pareto optimal microwave filter design using multiobjective differential evolution," *IEEE Trans. Antennas Propag.*, vol. 58, no. 1, pp. 132–144, Jan. 2010, doi: [10.1109/TAP.2009.2032100](https://doi.org/10.1109/TAP.2009.2032100).
- [26] J. Dobes, J. Michal, J. Popp, D. Cerny, M. Grabner, F. Vejrazka, J. Kakona, and S. Matejka, "Precise characterization and multiobjective optimization of low noise amplifiers," *Radioengineering*, vol. 24, no. 3, pp. 670–680, Sep. 2015, doi: [10.13164/re.2015.0670](https://doi.org/10.13164/re.2015.0670).
- [27] Y. Cengiz and E. Konar, "Pareto-optimal synthesis of microwave amplifier to design the noise-constrained gain value," *Microw. Opt. Technol. Lett.*, vol. 54, no. 4, pp. 1079–1084, Feb. 2012, doi: [10.1002/mop.26724](https://doi.org/10.1002/mop.26724).
- [28] J. Dobes, J. Michal, and V. Biolkova, "Multiobjective optimization for electronic circuit design in time and frequency domains," *Radioengineering*, vol. 22, no. 1, pp. 136–152 and 17, Apr. 2013.
- [29] F. Güneş and U. Özkaya, "Multiobjective FET modeling using particle swarm optimization based on scattering parameters with Pareto optimal analysis," *Turkish J. Elect. Eng. Comput. Sci.*, vol. 20, pp. 353–365, Apr. 2012.
- [30] F. Tokan and F. Güneş, "Pareto optimal synthesis of the linear array geometry for minimum sidelobe level and null control during beam scanning," in *Proc. Int. Conf. Electr. Eng.*, May 2010, vol. 7, no. 7, pp. 1–10.
- [31] E. Agastra, L. Lucci, R. Nesti, G. Pelosi, and S. Selleri, "Modified NSGA-II algorithm for multiobjective optimization of compact high-efficiency square horns," *Int. J. RF Microw. Comput.-Aided Eng.*, vol. 21, no. 2, pp. 174–181, Mar. 2011.
- [32] P. Singh, M. Rossi, I. Couckuyt, D. Deschrijver, H. Rogier, and T. Dhaene, "Constrained multi-objective antenna design optimization using surrogates," *Int. J. Numer. Model., Electron. Netw., Devices Fields*, vol. 30, no. 6, p. e2248, May 2017, doi: [10.1002/jnm.2248](https://doi.org/10.1002/jnm.2248).
- [33] K. Deb, A. Pratap, S. Agarwal, and T. Meyarivan, "A fast and elitist multiobjective genetic algorithm: NSGA-II," *IEEE Trans. Evol. Comput.*, vol. 6, no. 2, pp. 182–197, Apr. 2002, doi: [10.1109/4235.996017](https://doi.org/10.1109/4235.996017).
- [34] K. Deb and H. Jain, "An evolutionary many-objective optimization algorithm using Reference-Point-Based nondominated sorting approach, part I: Solving problems with box constraints," *IEEE Trans. Evol. Comput.*, vol. 18, no. 4, pp. 577–601, Aug. 2014, doi: [10.1109/TEVC.2013.2281535](https://doi.org/10.1109/TEVC.2013.2281535).
- [35] *Low Noise GaAs FET, HJ-FET*. Accessed: Dec. 7, 2019. [Online]. Available: <https://www.renesas.com/in/en/products/rf-devices/low-noise-gaas-fet-hj-fet/device/NE3511S02.html>.
- [36] A. M. Niknejad, "Lecture 9: Intercept point, gain compression and blocking," Univ. California, Berkeley, Berkeley, CA, USA, Tech. Rep. EECS 142, 2005.
- [37] S. A. K. Kahil, S. Laurent, R. Quere, J. Sombrin, D. Floriot, V. Brunel, and C. Teyssandier, "Linearity characterization of GaN HEMT technologies through innovative on-wafer multi-tone load-pull measurements," in *Proc. 11th Eur. Microw. Integr. Circuits Conf. (EuMIC)*, Oct. 2016, pp. 37–40, doi: [10.1109/EuMIC.2016.7777483](https://doi.org/10.1109/EuMIC.2016.7777483).
- [38] W. Guo and D. Huang, "The noise and linearity optimization for a 1.9-GHz CMOS low noise amplifier," in *Proc. IEEE Asia-Pacific Conf. (ASIC)*, Aug. 2002, pp. 253–257, doi: [10.1109/APASIC.2002.1031580](https://doi.org/10.1109/APASIC.2002.1031580).
- [39] T. H. Lee, *The Design of CMOS Radio-Frequency Integrated Circuits*. Cambridge, U.K.: Cambridge Univ. Press, 1998.
- [40] L. Lecheminoux and M. Villegas, "ACPR to third order interception point and 1 dB compression point new relationship," in *Proc. 30th Eur. Microw. Conf.*, Oct. 2000, pp. 1–4, doi: [10.1109/EUMA.2000.338635](https://doi.org/10.1109/EUMA.2000.338635).
- [41] R. E. Collin, *Foundations for Microwave Engineering*. New York, NY, USA: Wiley, 2007.
- [42] D. M. Pozar, *Microwave Engineering*. Hoboken, NJ, USA: Wiley, 2009.
- [43] F. Güneş and B. S. Yarman, "Potential broadband characteristics of a microwave transistor and realization conditions," in *Proc. PIERS Prog. Electromagn. Res. Symp.*, Cambridge, MA, USA, Jul. 2000, pp. 8–15.



FİLİZ GÜNEŞ received the M.Sc. degree in electronics and communication engineering from the Istanbul Technical University and the Ph.D. degree in communication engineering from the Bradford University, in 1979. Her current research interests are in the areas of multivariable network theory, device modeling, computer-aided microwave circuit design, monolithic microwave integrated circuits, and antenna designs.



AHMET ULUSLU received the M.Sc. degree in electronics and communication engineering from Yıldız Technical University, Istanbul, in 2013, where he is currently pursuing the Ph.D. degree with the Department of Electromagnetic Fields and Microwave Techniques. His current research interests are microwave circuits, especially optimization techniques of microwave circuits, programming aided circuit design, and microwave amplifiers.



PEYMAN MAHOUTI received the Ph.D. degree in electronics and communication engineering from Yıldız Technical University, in 2016. He is currently with Istanbul Cerrahpaşa University. His main research areas are analytical and numerical modeling of microwave devices, optimization techniques for microwave stages, and application of artificial intelligence-based algorithms.